Published in final edited form as:
Brain Res. 2010 June 25; 1342C: 118–126. doi:10.1016/j.brainres.2010.04.032.

Aldose reductase inhibition ameliorates the detrimental effect of estrogen replacement therapy on neuropathology in diabetic rats subjected to transient forebrain ischemia

Bin Shen[a,b], **Francesco Vetri**[b], **Lizhen Mao**[b], **Hao-Liang Xu**[b], **Chanannait Paisansthan**[b], and **Dale A. Pelligrino**[b,*]

[a] Department of Emergency Medicine, the First Affiliated Hospital of Nanjing Medical University, Nanjing, Jiangsu Province 210029, P.R. China

[b] Neuroanesthesia Research Laboratory, Department of Anesthesiology, University of Illinois at Chicago, 835 S Wolcott Street (M/C 513), Chicago, IL 60612, USA

Abstract

Estrogen replacement therapy (ERT) elicits a deleterious, instead of protective, effect on neuropathology in diabetic ovariectomized (OVX) rats subjected to cerebral ischemia. This transformation may be linked to an estrogen-associated increase in function of the receptor for advanced glycation end-products (RAGE). Moreover, under diabetic conditions, advanced glycation end-products (AGEs) are excessively generated through the aldose reductase (AR)-polyol pathway. As such, in diabetic rats given ERT, a RAGE-related exacerbation of post-ischemic brain injury can occur. Thus, in the present study, we evaluated the contribution of AR in estrogen's detrimental effect on diabetic animals subjected to transient forebrain ischemia (TFI). Streptozotocin- and 17-β estradiol-treated OVX female rats were divided into two groups, where AR activity was blocked using epalrestat; or AGEs production was restricted, via administrating the protein glycation crosslink breaker, ALT-711. In all animals, ERT was initiated ~10 days before TFI. Pial venular leukocyte adhesion was evaluated over 10 h post-TFI using a cranial window/intravital microscopy technique. In vehicle-treated control groups, a significant increase in leukocyte adhesion was observed post-TFI. Leukocyte extravasation, starting at ~6 h post-TFI, was detected in most of the control animals. Chronic administration of either epalrestat or ALT-711 was associated with a marked decrease in post-TFI leukocyte adhesion, and the complete prevention of leukocyte extravasation. Animals receiving either epalrestat or ALT-711 exhibited a significant improvement in neurologic function, at 72h post-ischemia, compared to vehicle-treated controls. Post-ischemic (72h) histopathology was significantly reduced by epalrestat. Compared to the non-diabetic (ND) controls, diabetic OVX rats in the absence or presence of ERT showed a significant 2-fold or 3-fold increase in cortical AR mRNA levels, respectively. In contrast, only a modest increase in AR protein expression, relative to ND control, was detected in the two diabetic groups. The present findings suggest that AR participates in estrogen's deleterious action on post-ischemic neuropathology in diabetics by promoting inflammation. Targeting the AR-controlled polyol pathway may be a clinically promising strategy to restore the neuroprotection of ERT in diabetic females.

* Correspondence: Dale A. Pelligrino, Neuroanesthesia Research Laboratory, Department of Anesthesiology, University of Illinois at Chicago, 835 S Wolcott Street (M/C 513), Chicago, IL 60612, USA, Tel: 312-996-1666, Fax: 312-355-1442, dpell@uic.edu.

Keywords

Cerebral ischemia; streptozotocin; ovariectomy; leukocyte; inflammation; receptor for advanced glycation end-products

Introduction

There is abundant evidence supporting the powerful neuroprotective and vasculoprotective actions of estrogen against cerebral ischemia, which is, at least partially, related to amelioration of post-ischemic inflammation (Santizo and Pelligrino, 1999; Wen et al., 2004). However, recent studies from our laboratory indicate that, in diabetic animals subjected to transient forebrain ischemia (TFI), estrogen no longer provides neuroprotection. Rather, the presence of estrogen is associated with neurotoxicity (Santizo et al., 2002; Xu et al., 2004; Xu et al., 2006). Evidence indicates that this conversion is mediated by the interaction of advanced glycation end-products (AGEs) with the receptor for advanced glycation end-products (RAGE), an interaction that is enhanced by estrogen (Xu et al., 2009). In diabetic tissue, accumulation of AGEs, the predominant RAGE ligand, occurs at an accelerated rate due to the elevated glycemia levels. The AGE-RAGE interaction causes intracellular oxidative stress, possibly via NADPH oxidase (Wautier et al., 2001), and the activation of the pro-inflammatory transcription factor, nuclear factor NFκB, via mitogen-activated protein kinase (MAP) and protein kinase C (PKC) signaling pathways. Encouraging results obtained in multiple studies indicate a beneficial effect of AGEs inhibition in diabetic animal models. Thus, among the various AGEs blockers, aldose reductase inhibitors (ARIs), such as epalrestat, have been shown to significantly decrease AGEs production (Tsukushi et al., 1999). Moreover, AR deletion has shown neuroprotective effects in cerebral ischemia in mice (Lo et al., 2007).

Aldose reductase is a monomeric NADPH-dependent enzyme. It is the first and rate-limiting enzyme of the polyol pathway that channels excess glucose to the formation of fructose. The polyol pathway plays a minor role in glucose metabolism in euglycemic conditions. However, during uncontrolled diabetes mellitus, an excessive amount of glucose is metabolized through this enzymatic cascade, thus providing potent precursors of AGEs. Furthermore, the subsequent high utilization of cofactors (such as NADPH) leads to a redox state imbalance. This situation may be further worsened by a second “hit” like an ischemic insult (Schmidt et al., 2000). Finally, Villablanca et al. (2002) reported a 17β-estradiol-associated elevation of AR mRNA expression in aortic endothelial cells, implying a possibly direct effect of estrogen on AR upregulation.

The present experiments were designed to address the hypothesis that, in the chronically hyperglycemic diabetic female, the AGE-RAGE-linked increased inflammation (Xu et al., 2009) and enhanced post-ischemic brain damage (Xu et al., 2006), associated with estrogen replacement therapy, arises from increased AR function. To that end, we examined post-TFI leukocyte adhesion/infiltration, and neuropathology in rats chronically treated with an aldose reductase inhibitor (epalrestat) or an agent (ALT-711) known to reduce accumulation of carboxymethyllysine-AGE—the most prevalent AGEs (Candido et al., 2003). In separate animals, we monitored cerebral cortical AR mRNA and protein expression. Significantly higher levels of AR mRNA (although not protein) were detected in the estrogen-replaced diabetic females. In addition, both epalrestat and ALT-711 chronic treatments yielded substantial anti-inflammatory and neuroprotective effects. These findings suggest that AR plays a key role in the enhanced post- ischemic neuroinflammation and neuropathology associated with estrogen replacement therapy in the diabetic female.

Results

Average plasma glucose levels reached 577 ± 6 mg/dl one week after streptozotocin (STZ) injection, which was significantly higher compared to non-diabetic controls (145 ± 10 mg/dl). The average daily water consumption for diabetic rats, at one week post-STZ, was over 400 $ml.kg^{-1}$ compared to the ~100 $ml.kg^{-1}.day^{-1}$ consumed by non-diabetics. The increased glucose level and the diabetic symptoms persisted during the experimental period. Thus, 6 weeks after STZ injection, the average glucose level was 508 ± 68 mg/dl, and animals consumed as much as 6 times more water than their controls. No significant change was observed with respect to the plasma glucose concentration and diabetic symptoms during epalrestat or ALT-711 treatment, so that treatment effects cannot be attributed to changes in glycemia.

Effects of epalrestat and ALT-711 on post-ischemic leukocyte behavior in E_2-treated OVX diabetic rats

In agreement with our previous studies (Xu et al., 2006), *intravascular* leukocyte adhesion in diabetic, vehicle-treated, and E_2-supplemented OVX females showed a progressive increase during the 10 h post-TFI observation period (Fig. 1A,B). Epalrestat treatment (Fig. 1A) was associated with significantly lower levels of intravascular leukocyte adhesion over the 6-10h reperfusion interval (~40-50% less than controls). As previously mentioned, accumulation of AGEs in the cerebral cortex has been identified as a relevant factor contributing to estrogen's neuropathologic actions in diabetics exposed to ischemia and reperfusion (Xu et al., 2009). Chronic treatment with ALT-711 has been shown to reverse already formed AGE-crosslinking in diabetic animals and reduce accumulation of carboxymethyllysine-AGE (Candido et al., 2003). If the AR-controlled enzymatic cascade is a predominant source of AGEs generation, ALT-711 would be expected to display similar effects as epalrestat. To confirm this hypothesis, ALT-711 was introduced as an alternative strategy to decrease AGEs accumulation. Post-TFI intra-venular leukocyte adhesion in the presence of ALT-711 was significantly reduced relative to vehicle control rats (by ~75% at 6-10h reperfusion; Fig 1B). Also, as observed in earlier studies from our laboratory (Xu et al., 2009), vehicle controls exhibited an extravascular presence of leukocytes beginning approximately at 6 h of reperfusion. To quantitate leukocyte transmigration, an “index of leukocyte infiltration” was calculated as described in the Methods. Since results were similar, data from both *vehicle* groups were combined. Thus, the index values (the leukocyte area outside the vessel expressed as a percentage of the viewed venular area) at 6, 8, and 10h post TFI were 6.5 ± 2.8%, 9.5 ± 2.4%, and 13.2 ± 2.6%, respectively. Based upon a comparison between the total (intra- plus extra-vascular) leukocyte presence vs the intravascular leukocyte presence, the 8 and 10h values were found to be statistically significant. In contrast to vehicle-treated controls, no leukocyte extravasation was detected during the entire observation period in either epalrestat- or ALT-711-treated rats (fig. 1D-E). Taken together, these results suggest that, in diabetic rats, polyol pathway-derived AGEs play a key role in reversing estrogen's normally counter-inflammatory and neuroprotective actions.

Neurologic outcomes

Post-ischemic neurological deficit scores in the presence of epalrestat, ALT-711, or vehicle treatment are summarized in Fig 2. Since both vehicle control groups had virtually identical median values, the control data was pooled. Both epalrestat and ALT-711 treatments significantly improved post-ischemic neurological outcome, compared to their age-matched vehicle controls. The median (5^{th}-95^{th} percentiles) neurologic score values were 22 (5-46), 5 (2-20), and 6 (2-21) in the pooled control, epalrestat, and ALT-711 groups, respectively.

Histopathology

FluoroJade B staining was conducted in epalrestat-treated diabetic OVE_2 rats to examine the effect of AR inhibition on TFI-induced neuronal degeneration. Consistent with our previous

results (Xu et al., 2006), brain sections harvested from vehicle-treated animals showed high-density FJB reactivity throughout the cortex, striatum and hippocampus in the ischemic hemisphere (fig. 3A-C). A scattering of FJB-positive neurons were also found in the dorso-medial thalamus (not shown). No FJB-positive neurons were detected in the contralateral hemisphere. Epalrestat largely prevented the TFI-induced neuronal damage in cortex, striatum, and hippocampus, as indicated by a relative absence of FJB-positive cells in those regions (fig. 3D-F). Figure 4 provides a quantitative representation of degenerating neurons in the cortex, striatum, and hippocampus. Counts were obtained from coronal sections obtained at 72h reperfusion, as described in the Methods. Relative to controls, substantially fewer (by >90%; $p<0.05$) FJB-positive neurons in the cortex, striatum, and hippocampus were observed in epalrestat-treated rats.

mRNA and protein analyses

The relative value of GADPH mRNA expression for each individual sample was used as a reference for AR mRNA expression. Compared to OVX+ND controls, cortical tissue from the OVX+DM group exhibited a much higher AR mRNA expression value (0.42 ± 0.14 for OVX +DM *vs* 0.17 ± 0.02 for OVX+ND, $p<0.05$) (fig. 5A.). An even greater relative AR mRNA expression was observed in the OVE_2+DM group (0.64 ± 0.02). These mRNA changes, however, were not strictly mirrored by the protein expression patterns. Thus, both diabetic groups displayed a 23-24% higher AR (relative to β-actin) expression, compared to OVX+ND females. The one-way analysis of variance on ranks revealed a statistically significant difference ($p=0.04$) among the 3 groups. This probably reflected a difference between diabetic and non-diabetic animals. However, no statistical significance was detected in post hoc comparisons of the OVX+DM, OVE_2+DM, and OVX+ND groups to one another (Fig 5B).

Discussion

Studies from our laboratory indicated that, in diabetic, as opposed to non-diabetic, animals subjected to TFI, estrogen is converted from a neuroprotective to a neurotoxic substance (Santizo et al., 2002; Xu et al., 2006). That transformation was characterized by an enhanced rather than diminished, post-ischemic leukocyte adhesion and cerebral infiltration in diabetic OVX rats given ERT (Xu et al., 2004; Xu et al., 2006). Evidence accumulated in our laboratory (Xu et al., 2006), and others (Frijns and Kappelle, 2002), suggests that the appearance of leukocytes within the brain leads to neuronal damage. Oxidative stress has been proposed as one key mechanism contributing to the damaging effects of leukocytes (Wong and Crack, 2008). However, others have argued against a primary post-ischemic pathologic role for leukocytes (e.g., Emerich et al., 2002). Nevertheless, based on our studies (Santizo et al., 2002; Xu et al., 2004; Xu et al., 2009), the post-ischemic leukocyte accumulation in ischemic brain areas, especially in estrogen-exposed diabetic females, is accompanied by pronounced neuropathology. For instance, the extent of ischemic damage, assessed after several days of post-ischemic reperfusion, seems to reflect the extent of leukocyte (mostly neutrophil) recruitment over the initial 10h or so of reperfusion. Additional evidence that this leukocyte activity is linked to brain damage arises from studies employing anti-neutrophil antibody-induced neutropenia, which yields significant improvement in both neuropathology and neurologic function (Xu et al., 2006). The correlation between post-ischemic leukocyte invasion and neuropathology in the current study is in agreement with previously reported results from our laboratory (Xu et al., 2006). That correlation was also maintained when viewed in the opposite direction. That is, the suppression of leukocyte activity (over 10h post-TFI), that accompanied both epalrestat and ALT-711 treatments, was paralleled by an improvement in neurologic outcomes and a more limited neuronal damage assessed over 72h reperfusion.

Diabetes-associated pro-inflammatory changes oppose the counter-inflammatory and neuroprotective actions of estrogen. However, while the pro-inflammatory effect of diabetes might account for a weakening of estrogen's neuroprotective influence, it does not explain the greater post-ischemic leukocyte adhesion/infiltration and neuropathology in estrogen-exposed (E_2-replaced OVX and intact diabetic females) (see Xu et al., 2009), compared to untreated OVX diabetic rats. A likely explanation may be found in a recent paper from our laboratory (Xu et al., 2009). In that study, we reported evidence of an increased function of the receptor for advanced glycation endproducts (RAGE) in cortical tissue of diabetic rats receiving ERT. Thus, an E_2-related increased expression and/or activity of RAGE, coupled with a hyperglycemia-linked enhanced presence of its ligand, AGEs, may promote a significant increase in leukocyte-related post-ischemic inflammatory activity (Dukic-Stefanovic et al., 2003; Nitti et al., 2007). Thus, the enhanced RAGE-related signaling pathway would not only interfere with the beneficial effects of estrogen, but also exacerbate brain injury.

During diabetes, glucose channeled through the AR pathway can become excessive (Yabe-Nishimura, 1998). The subsequent depletion of cellular NADPH may hamper the regeneration of glutathione and alter the cellular redox balance, thus increasing the susceptibility to oxidative stress. Of particular relevance to the present investigation, the direct phosphorylation of the sorbitol metabolite, fructose, by fructose-3-phosphokinase generates fructose-3-phosphate, which can lead to the formation of 3-deoxyglucosone, a key intermediate known to accelerate the formation of AGEs (Kaneko et al., 2005). Besides the increased amount of substrate, an enhanced expression (at both the translational and transcriptional level) and activity of AR have been reported in diabetic animals (Chandra et al., 2002; Dan et al., 2004; Ghahary et al., 1991; Yabe-Nishimura, 1998). Thus, an excessive amount of AR-derived AGEs may accumulate over time due to an increased driving force through the AR pathway.

Interestingly, findings from recent reports have indicated that acute treatments with an AR inhibitor in non-diabetic rodents prevented post-ischemic inflammation (Agardh et al., 2009) and injury (Cheung et al., 2007) in the retina. This suggests that chronic diabetes is not the only condition linked to AR-related pro-inflammatory/cytotoxic influences. But, acute inhibition of sorbitol dehydrogenase (SDH), which blocks sorbitol to fructose conversion and subsequent AGEs generation, was without any benefit in retinal ischemia/reperfusion (Cheung et al., 2007). These limited findings suggest that the AR-related mechanism of acute post-ischemic damage (at least in the retina) does not involve the principal AGE-generating arm of the AR pathway, distal to SDH. If the same mechanisms were at play in the present study, one might expect a benefit from epalrestat, but not ALT-711. Furthermore, in several pilot experiments in our laboratory, where epalrestat was administered to OVE_2+DM females just prior to ischemic onset, no neurologic improvement was noted over a 3-day reperfusion (data not shown). This is consistent with findings in ***diabetic*** animals showing that the benefits afforded by AR inhibitors and ALT-711 (e.g., vasculoprotection) appear to require many weeks of drug exposure (Demiot et al., 2006). The need for extended treatment and the fact that both drugs were effective supports a diabetes-specific pathology involving AGEs.

There are several pieces of evidence that could be taken to support, at least circumstantially, a linkage, in diabetic rats, between enhanced AR function, AGEs generation, and the presence of E_2, in the promotion of enhanced post-ischemic inflammation in the brain. First, we recently reported a substantial increase in the accumulation of carboxymethyllysine-AGE, that was especially concentrated in perivascular elements of cortical tissue of diabetic rats (Xu et al., 2009), with the highest level of AGEs being detected in OVX diabetic female rats with ERT (about 4-fold higher, when compared to untreated diabetic OVX females). Second, in the present study, AR mRNA expression in the cerebral cortex of diabetic E_2-treated OVX rats was significantly higher than in untreated OVX diabetic rats. Third, bearing some similarity to our findings, Villablanca et al. (Villablanca et al., 2002) reported an estrogen-induced

increase in AR mRNA expression in cultured endothelial cells. On the other hand, AR protein expression, in our study, was not affected to the same degree as mRNA. A weak correlation between mRNA and protein abundance is not uncommon in the literature (e.g., Nie et al., 2006; Xu et al., 2009). Many posttranscriptional factors, such as translational regulation, posttranslational modification, and protein degradation, may influence mRNA and protein expression comparisons. Nevertheless, in the current investigation, both chronic AR blockade, and ALT-711-related restriction of AGEs cross-linking and accumulation, repressed post-ischemic leukocyte behavior and were associated with brain protection. This raises the possibility that estrogen's post-ischemic pro-inflammatory and neurotoxic influence in diabetic rats may involve multiple mechanisms (e.g., increased RAGE function and enhanced generation of AGEs).

In conclusion, over the long term, both inhibition of AR activity and reducing the presence of AGEs yielded similar results—i.e., restriction of leukocyte recruitment and reduced brain damage. This implies that AR-linked AGEs may play an important role in the enhanced neuropathology observed in diabetic OVX females given ERT. It is clinically relevant to explore the mechanisms involved in the deleterious effects of hormone replacement therapy on ischemic neuropathology in diabetic subjects. That is, although there may not be a causal link, in women at the age of menopause onset, diabetic symptoms often appear as well.

Methods and Materials

Animal

The study protocol was approved by the Institutional Animal Care and Use Committee. Ovariectomized (OVX) female Sprague-Dawley rats (200-250 g at arrival) were used for this study. Ovariectomies were performed by the vendor (Charles River) one week prior to shipment. Diabetes was induced via streptozotocin (60 mg/kg, i.v.) 1 week following animal arrival, and the rats were studied 8 weeks later. Animals received chronic 17β-estradiol (E_2) treatment (0.1 $mg.kg^{-1}.day^{-1}$ for 10~14 days, i.p.) starting at 10 to 14 days prior to TFI. Previous results from our lab have demonstrated that 0.1 $mg.kg^{-1}.day^{-1}$ of E_2 *i.p.* results in an average daily plasma E_2 concentration that falls between the peak and nadir levels observed over the normal rat estrous cycle (Wang et al., 1999).

Experimental preparation and protocol

Diabetic OVX rats with ERT were selected for the study. These animals were divided into two groups based on two different pharmacological interventions: epalrestat (AR inhibitor) treatment (50 $mg.kg^{-1}.day^{-1}$, dissolved in 5 % Arabic gum—from Haorui Pharma-Chem, Edison, NJ); ***and*** protein glycation crosslink breaker, ALT-711, treatment (10 $mg.kg^{-1}.day^{-1}$, dissolved in saline—obtained from Alteon, Inc., Parsippany, NJ). Both drugs were administered to animals via oral gavage. These treatments were started right after the establishment of diabetes and maintained throughout. The age matched vehicle-treated controls received 5% Arabic gum or saline. On the experimental day, rats were anesthetized with isoflurane. Paralysis was then induced with curare, followed by mechanical ventilation. The femoral arteries and veins were cannulated for blood sampling, arterial pressure monitoring, and drug infusions. Rectal temperature was servo-controlled at 37°C with a heating pad. The right common carotid artery was isolated for later clamping, followed by insertion of a right subclavian venous catheter. Forty min prior to TFI, isoflurane was replaced by fentanyl (10 $\mu g.kg^{-1}$ loading dose), and anesthesia was then maintained with 25 $\mu g.kg^{-1}.h^{-1}$ fentanyl / 70 % N_2O / 30 % O_2. Transient forebrain ischemia was produced by unilateral carotid clamping combined with hemorrhagic hypotension. Blood withdrawal was adjusted in order to reduce and maintain cortical blood flow on the clamped side at 20 % of the baseline (as measured by laser Doppler flowmetry) for 20 min. At the end of ischemia, the carotid clamp was removed

and the withdrawn blood was slowly re-infused, over a 15-min period. Animals were then prepared for cranial window installation. The head was stabilized in a stereotaxic frame, and a 10 mm diameter craniotomy performed over the skull midline. After carefully removing the dura, a glass window outfitted with three ports was mounted for pial vessel and leukocyte observation (Xu et al., 2004). The space under the cranial window was suffused with artificial cerebrospinal fluid (aCSF) at 0.5 ml.min^{-1}. Temperature, mean arterial blood pressure (MABP), and intracranial pressure (ICP) were monitored and maintained within normal limits. A microscope was positioned over the window and focused on pial venules measuring 50~80 μm in diameter. The vessels were displayed on a computer monitor at ~800× their actual size.

Leukocyte monitoring

Leukocytes labeled with rhodamine 6G (Xu et al., 2004) were monitored for 10 h post-TFI via a rhodamine-filtered monochromatic digital camera (CoolSnap ES, Photometrics, Tucson, AZ). A video record of each experiment was made for subsequent analysis of leukocyte adhesion using MetaMorph software (Universal Imaging Corporation, Downington, PA). Leukocyte adhesion was evaluated as the percentage of adherent leukocytes occupying the viewed venular area in the microscopic field. In those cases where the presence of extra-vascular leukocytes was observed (i.e. leukocyte infiltration), the total area of intra- and extra-vascular leukocyte presence was expressed in relation to the viewed venular area. The difference between these values (i.e., total leukocyte presence) ***and*** the adherent (intra-vascular) leukocyte percentages at equivalent time points in each animal was then calculated. This provided us with an “index of leukocyte infiltration” (see Xu et al., 2009).

Neurobehavioral assessments

Neurological outcome assessments were performed in some animals in these groups. In such cases, the cranial window implantation procedure was omitted. Thus, at the end of the ischemia/reperfusion, the catheters were removed and skin over all wound sites was infiltrated with bupivacaine and sutured. Muscle relaxant and anesthesia were discontinued. After spontaneous breathing was re-established, animals were extubated and returned to their cages. The rats were subjected to neurologic deficit evaluations at 24, 48 and 72 h post-TFI. The neurological outcome scoring methodology, based upon the sum of the 24, 48, and 72h scores, was described in a previous report from our laboratory (Santizo et al., 2002). A 17-point scale was used. There were 6 different categories: (1) consciousness (scores range from 0 [normal] to 4 [seizures]); (2) rope platform (scores range from 0 [climbs to platform] to 4 [no grasp reflex]); (3) limb tone (normal=0, weak=1); (4) walking (scores range from 0 [normal] to 4 [unable to stand]); (5) rotating screen, for which the range is 0 (grasps to 80° >5 seconds) to 3 (falls from vertical screen); and (6) pain reflex (normal=0, hypoactive=1). A summed daily score of 0 would indicate no dysfunction. Rats that did not regain consciousness after ischemia or failed to survive at least 48 h post-ischemia were excluded. The rationale for this exclusion was that it was seldom possible to establish, with any confidence, whether death was caused by CNS or non-CNS factors, unless one fortuitously witnessed a neurologic “event” (e.g., seizure) just prior to death. For rats surviving >48h, but <72h, we extrapolated a 72h value from the mean of the 24 and 48h scores. It should be noted that there were few rats, in the 4 experimental groups, which were included based upon the above criterion (2 epalrestat vehicle controls, 1 ALT-711 vehicle control, 1 epalrestat-treated, and 0 ALT-711-treated). Rats that failed to survive at least 48h were also few in number: 0 epalrestat vehicle controls; 2 ALT-711 vehicle controls; 0 epalrestat-treated; and 1 ALT-711-treated.

Histopathology

After the neurological assessments, rats were sacrificed and transcardially perfused with cold phosphate-buffered saline (PBS) followed by 20 ml paraformaldehyde. Brains were harvested

and paraffin-embedded. Coronal sections (7 μm) were obtained and prepared for Fluoro-Jade B (FJB) staining as we previously described (Xu et al., 2006). Brain sections were viewed through a fluorescence microscope (Nikon, Melville, NY), and images from the ischemic cortex, striatum, thalamus and hippocampus were captured using a Spot 2 digital camera and the MetaMorph software. Fluoro-Jade B-positive cells in 3 optical fields for each brain region were counted for comparison (Xu et al., 2006).

Aldose reductase mRNA and protein measurements

To examine whether AR expression levels in brain tissue may be affected by both diabetes and ERT, additional animals were assigned to three groups: ovariectomized non-diabetic females (OVX+ND); ovariectomized diabetic females (OVX+DM); and ovariectomized diabetic females with 10~14 days ERT (OVE_2+DM). These rats were not subjected to cerebral ischemia. In preparation for brain sampling, all rats were giveng an isoflurane overdose, followed by transcardial perfusion with cold PBS. Cortical tissue was removed, snap frozen in liquid nitrogen, and stored at −80 °C until the time of use. For RT-PCR, cortical tissue was homogenized in TRIZOL reagent (50 mg tissue to 1 ml Trizol reagent, Invitrogen) using a glass-Teflon homogenizer, and total RNA was isolated in accordance with standard protocols. To ensure that equal amounts of RNA were used for each reaction, the expression of glyceraldehyde-3-phosphate dehydrogenase (GAPDH) was used as an internal control (or reference gene) for each reaction. Gene-specific primers for AR and GAPDH were purchased from Integrated DNA Technologies (Coralville, Iowa). The sequences of the sense and antisense primers were 5′-ACTGCCATT GCAAAGGCATCGTGGT-3′ and 5′-CCCCCATAGGACTGGAGTTCTAAGC-3′, respectively, for detecting rat AR mRNA; ***and*** 5′-AGACAGCCGCATCTTCTTGT-3′, and 5′-CCACAGTCT TCTGAGTGGCA-3′, respectively, for rat GAPDH. RT-PCR was conducted according to the manufacturer's instructions (SuperScript™ III One-Step RT-PCR System, Invitrogen), with 25 cycles for AR and 23 cycles for GAPDH. Cycling conditions were: initial denaturation at 94 °C for 3 min, followed by 94 °C for 30 s, 53 °C for 40 s, 72 °C for 40 s, and a final extension of 72 °C for 5 min. PCR products were run on 1% agarose gel and visualized by ethidium bromide staining. Amounts were quantified by measuring the intensity of light emitted from corresponding bands under UV light. Image J software (NIH) was used for RT-PCR image analysis. The results were expressed as the ratio of the intensities of AR and GAPDH bands to correct any differences in the starting amount of RNA. To examine the protein expression changes of AR, the same set of brain samples were processed for Western blot according to a protocol previously described (Xu et al., 2009). The blot was hybridized with goat anti-mouse aldose reductase polyclonal antibody (1:100) (P-20, Santa Cruz Biotechnology, Santa Cruz, CA), and subsequently incubated with donkey anti-goat antibody conjugated with infrared dye (IRDye 680, LI-COR Biosciences, Lincoln, NE) diluted 1:5000 in 0.5× Odyssey blocking buffer and 0.1% Tween 20. β-actin was used as a loading control (mouse anti β-actin monoclonal, 1:2000, Sigma; rabbit anti-mouse, 1:10000, IRDye 800, Rockland Immunochemicals, Philadelphia, PA). Blot membranes were then scanned using the Licor Odyssey Infrared Imaging System (LI-COR Biosciences, Lincoln, NE). The protein level of AR in each brain sample (n=4 in each group) was expressed as the ratio of the optical densities of AR and β-actin bands. The average of the ratios from 3 different membranes for each brain sample was used for statistical comparison between groups.

Plasma glucose concentrations were measured using a 2300 STAT glucose analyzer from Yellow Springs Instruments (Yellow Springs, OH). Blood PO_2, PCO_2, and pH were measured using a Radiometer Copenhagen Blood Gas Analyzer (Model ABL520, Radiometer Medical, Copenhagen, Denmark).

Results were presented as means ± SE, unless otherwise noted. Several statistical analyses were used. For comparisons of intravascular adhesion (in drug- vs vehicle-treated rats) and histopathology data, a one-way analysis of variance (ANOVA), combined with a *post hoc* Tukey analysis was used. For neurologic outcome, mRNA, and protein results, a Kruskal-Wallis one-way ANOVA on ranks was used, and a *post hoc* Dunn's test was applied. A one-way repeated-measures ANOVA was utilized in the analysis of leukocyte infiltration data. In this instance, the total (intra- plus extra-vascular) leukocyte presence was compared to the intravascular leukocyte presence, both expressed as a percentage of the viewed venular area. $p < 0.05$ was considered significant.

Acknowledgments

This study was supported by grants 1R01DK65629 and RO1HL88259 from the National Institutes of Health (DAP), grant 0635337N from American Heart Association (HLX), and grant 3-2008-462 from the Juvenile Diabetes Research Foundation (FV). The authors wish to thank Alteon Inc. for the gift of ALT-711, and Susan Anderson for her expert technical assistance.

References

Agardh CD, Agardh E, Obrosova IG, Smith ML. The aldose reductase inhibitor fidalrestat suppresses ischemia-reperfusion-induced inflammatory response in rat retina. Pharmacology 2009;84:257–263. [PubMed: 19776662]

Candido R, Forbes JM, Thomas MC, Thallas V, Dean RG, Burns WC, Tikellis C, Ritchie RH, Twigg SM, Cooper ME, Burrell LM. A breaker of advanced glycation end products attenuates diabetes-induced myocardial structural changes. Circ Res 2003;92:785–792. [PubMed: 12623881]

Chandra D, Jackson EB, Ramana KV, Kelley R, Srivastava SK, Bhatnagar A. Nitric oxide prevents aldose reductase activation and sorbitol accumulation during diabetes. Diabetes 2002;51:3095–3101. [PubMed: 12351453]

Cheung AK, Lo AC, So KF, Chung SS, Chung SK. Gene deletion and pharmacological inhibition of aldose reductase protect against retinal ischemic injury. Exp Eye Res 2007;85:608–616. [PubMed: 17727843]

Dan Q, Wong R, Chung SK, Chung SS, Lam KS. Interaction between the polyol pathway and non-enzymatic glycation on aortic smooth muscle cell migration and monocyte adhesion. Life Sci 2004;76:445–459. [PubMed: 15530506]

Demiot C, Fromy B, Saumet JL, Sigaudo-Roussel D. Preservation of pressure-induced cutaneous vasodilation by limiting oxidative stress in short-term diabetic mice. Cardiovasc Res 2006;69:245–252. [PubMed: 16266692]

Dukic-Stefanovic S, Gasic-Milenkovic J, Deuther-Conrad W, Munch G. Signal transduction pathways in mouse microglia N-11 cells activated by advanced glycation endproducts (AGEs). J Neurochem 2003;87:44–55. [PubMed: 12969251]

Emerich DF, Dean RL III, Bartus RT. The role of leukocytes following cerebral ischemia: pathogenic variable or bystander reaction to emerging infarct? Exp Neurol 2002;173:168–181. [PubMed: 11771949]

Frijns CJ, Kappelle LJ. Inflammatory cell adhesion molecules in ischemic cerebrovascular disease. Stroke 2002;33:2115–2122. [PubMed: 12154274]

Ghahary A, Chakrabarti S, Sima AA, Murphy LJ. Effect of insulin and statil on aldose reductase expression in diabetic rats. Diabetes 1991;40:1391–1396. [PubMed: 1936600]

Kaneko M, Bucciarelli L, Hwang YC, Lee L, Yan SF, Schmidt AM, Ramasamy R. Aldose reductase and AGE-RAGE pathways: key players in myocardial ischemic injury. Ann N Y Acad Sci 2005;1043:702–709. [PubMed: 16037296]

Lo AC, Cheung AK, Hung VK, Yeung CM, He QY, Chiu JF, Chung SS, Chung SK. Deletion of aldose reductase leads to protection against cerebral ischemic injury. J Cereb Blood Flow Metab 2007;27:1496–1509. [PubMed: 17293845]

Nie L, Wu G, Zhang W. Correlation of mRNA expression and protein abundance affected by multiple sequence features related to translational efficiency in Desulfovibrio vulgaris: a quantitative analysis. Genetics 2006;174:2229–2243. [PubMed: 17028312]

Nitti M, Furfaro AL, Traverso N, Odetti P, Storace D, Cottalasso D, Pronzato MA, Marinari UM, Domenicotti C. PKC delta and NADPH oxidase in AGE-induced neuronal death. Neurosci Lett 2007;416:261–265. [PubMed: 17317001]

Santizo R, Pelligrino DA. Estrogen reduces leukocyte adhesion in the cerebral circulation of female rats. J Cereb Blood Flow Metab 1999;19:1061–1065. [PubMed: 10532629]

Santizo RA, Xu HL, Ye S, Baughman VL, Pelligrino DA. Loss of benefit from estrogen replacement therapy in diabetic ovariectomized female rats subjected to transient forebrain ischemia. Brain Res 2002;956:86–95. [PubMed: 12426050]

Schmidt AM, Yan SD, Yan SF, Stern DM. The biology of the receptor for advanced glycation end products and its ligands. Biochim Biophys Acta 2000;1498:99–111. [PubMed: 11108954]

Tsukushi S, Katsuzaki T, Aoyama I, Takayama F, Miyazaki T, Shimokata K, Niwa T. Increased erythrocyte 3-DG and AGEs in diabetic hemodialysis patients: role of the polyol pathway. Kidney Int 1999;55:1970–1976. [PubMed: 10231461]

Villablanca AC, Lewis KA, Rutledge JC. Time- and dose-dependent differential upregulation of three genes by 17 beta-estradiol in endothelial cells. J Appl Physiol 2002;92:1064–1073. [PubMed: 11842041]

Wang Q, Santizo R, Baughman VL, Pelligrino DA. Estrogen provides neuroprotection in transient forebrain ischemia through perfusion-independent mechanisms in rats. Stroke 1999;30:630–637. [PubMed: 10066863]

Wautier MP, Chappey O, Corda S, Stern DM, Schmidt AM, Wautier JL. Activation of NADPH oxidase by AGE links oxidant stress to altered gene expression via RAGE. Am J Physiol Endocrinol Metab 2001;280:E685–E694. [PubMed: 11287350]

Wen Y, Yang S, Liu R, Perez E, Yi KD, Koulen P, Simpkins JW. Estrogen attenuates nuclear factor-kappa B activation induced by transient cerebral ischemia. Brain Res 2004;1008:147–154. [PubMed: 15145751]

Wong CH, Crack PJ. Modulation of neuro-inflammation and vascular response by oxidative stress following cerebral ischemia-reperfusion injury. Curr Med Chem 2008;15:1–14. [PubMed: 18220759]

Xu HL, Baughman VL, Pelligrino DA. Estrogen replacement treatment in diabetic ovariectomized female rats potentiates postischemic leukocyte adhesion in cerebral venules. Stroke 2004;35:1974–1978. [PubMed: 15232125]

Xu HL, Salter-Cid L, Linnik MD, Wang EY, Paisansathan C, Pelligrino DA. Vascular adhesion protein-1 plays an important role in postischemic inflammation and neuropathology in diabetic, estrogen-treated ovariectomized female rats subjected to transient forebrain ischemia. J Pharmacol Exp Ther 2006;317:19–29. [PubMed: 16339390]

Xu HL, Vetri F, Lee HK, Ye S, Paisansathan C, Mao L, Tan F, Pelligrino DA. Estrogen replacement therapy in diabetic ovariectomized female rats potentiates postischemic leukocyte adhesion in cerebral venules via a RAGE-related process. Am J Physiol 2009;297:H2059–H2067.

Yabe-Nishimura C. Aldose reductase in glucose toxicity: a potential target for the prevention of diabetic complications. Pharmacol Rev 1998;50:21–33. [PubMed: 9549756]

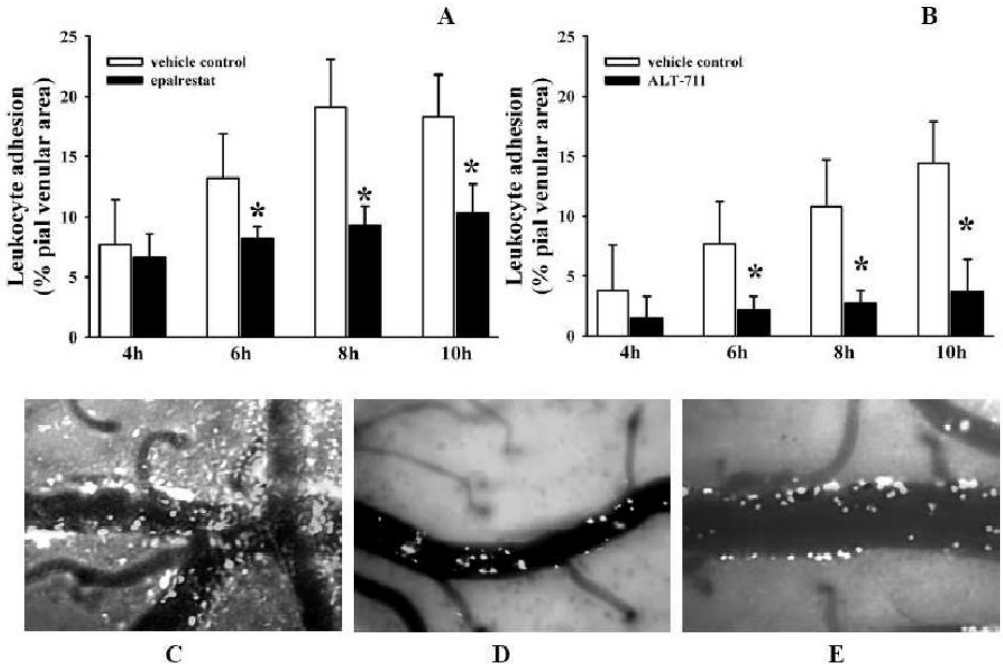

Fig 1.

Effects of the aldose reductase inhibitor, epalrestat **(A)**, and the protein glycation crosslink breaker, ALT-711 **(B)**, on post-ischemic venular leukocyte adhesion in ovariectomized diabetic rats with estrogen replacement therapy. Either epalrestat or ALT-711 treatment was initiated right after the establishment of streptozotocin-induced diabetes, and maintained for 6 weeks, until the completion of the experiment. Leukocyte adhesion was observed from 4 to 10 h of reperfusion, following 20 min of transient forebrain ischemia. Results in panels A and B are represented as the area percentage of adherent leukocytes occupying the viewed intravascular venular area. *$p<0.05$ *vs* vehicle treated controls. n=5 in each group. A representative pattern of leukocyte adhesion/infiltration in a vehicle control is provided in panel C (depicts extravasated leukocytes at 10h reperfusion). Panels D and E represent typical leukocyte behavior in epalrestat and ALT-711-treated rats, respectively—i.e., reduced intravascular adhesion and a lack of extravasation at 10h reperfusion,

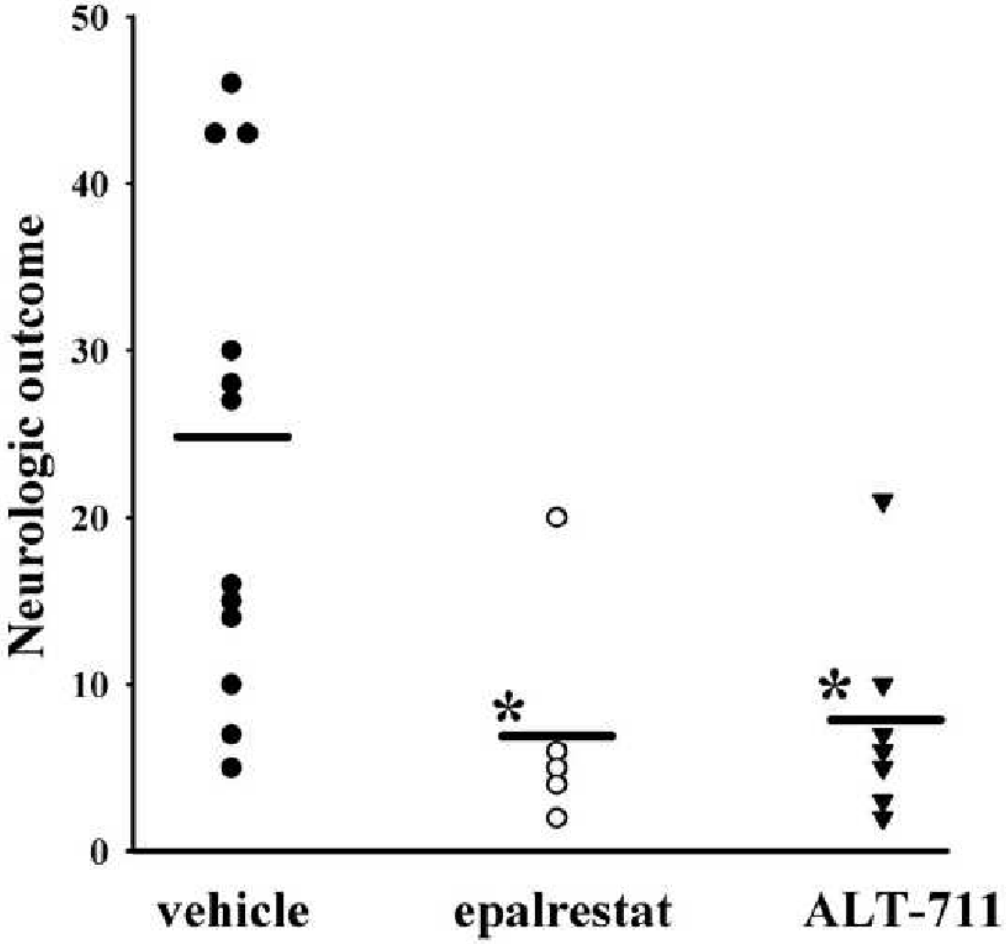

Fig 2.

Neurological outcome assessment on rats receiving 6-week treatment of either the aldose reductase inhibitor, epalrestat; the protein glycation crosslink breaker, ALT-711; or vehicle, followed by 20 min transient forebrain ischemia (TFI) and 72h reperfusion. All animals were diabetic, ovariectomized, and treated with E_2. Each datapoint in the scatter plot represents the sum of the neurological scores (see Methods) obtained at 24, 48, and 72h post-TFI for any evaluated animal. The vehicle control results represent the pooled data from both control groups. The horizontal lines represent the median values for each experimental group. *$p<0.05$ *vs* vehicle-control group.

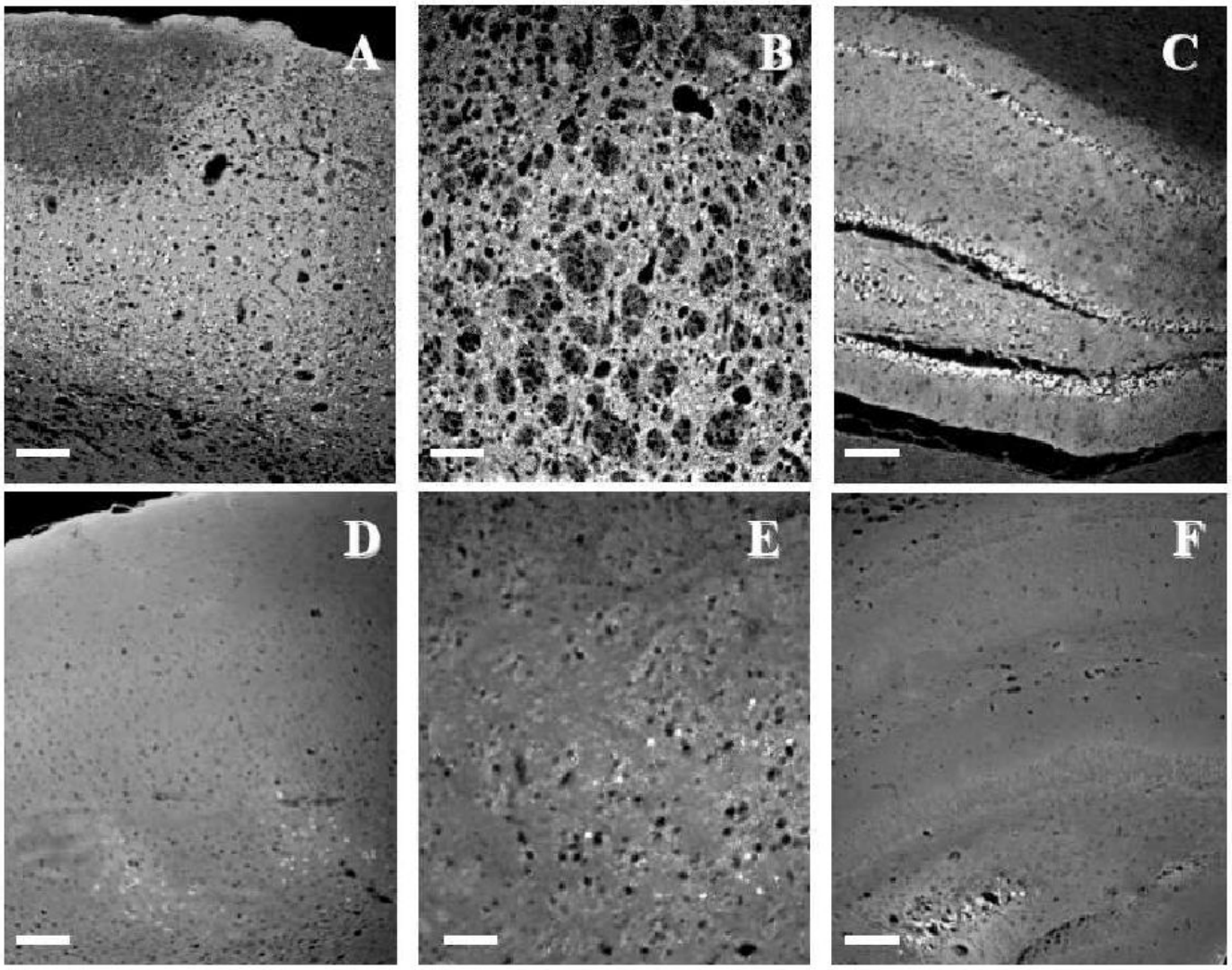

Fig 3.

Representative photomicrographs obtained at 72h reperfusion in vehicle- and epalrestat-treated rats. Panels A-C show FluoroJade B (FJB)-positive (degenerating) neurons in the cortex, striatum and hippocampus of vehicle-treated animals; while panels D-F show FJB-positive neurons within the same regions of epalrestat-treated animals. Scale bars = 100 μm.

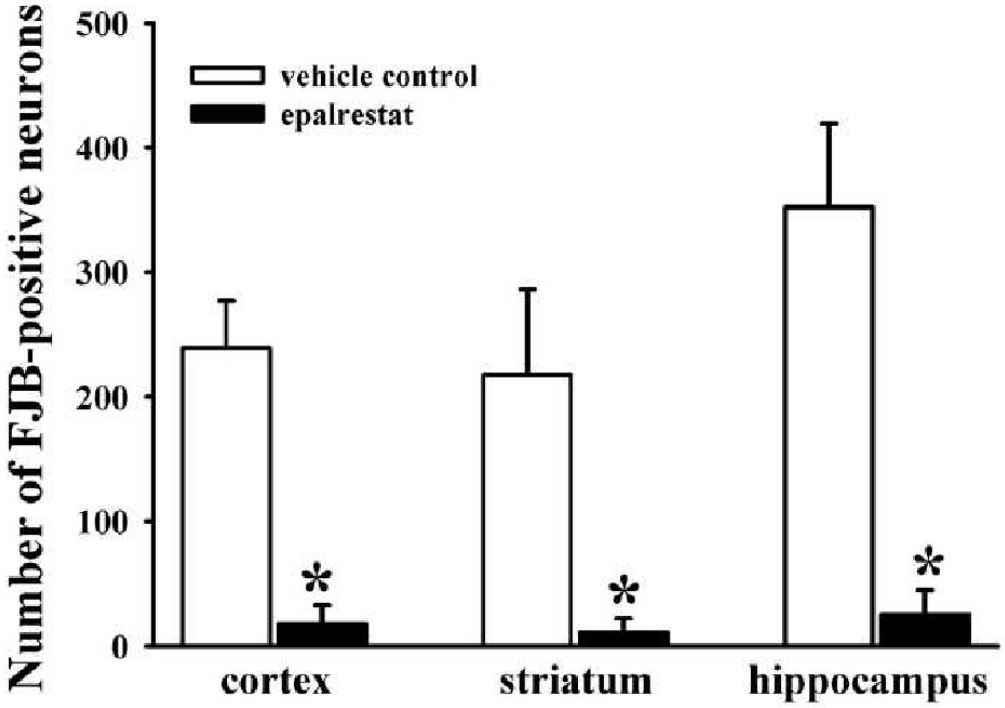

Fig. 4.

Quantitative evaluations of degenerating (FJB-positive) neurons within the three brain regions depicted in fig. 3. Counts for each region were obtained from coronal sections at comparable levels relative to bregma in epalrestat- and vehicle-treated rats. Values are means ± SE; *$p<0.05$ *vs* vehicle control; n=3-4 in each group.

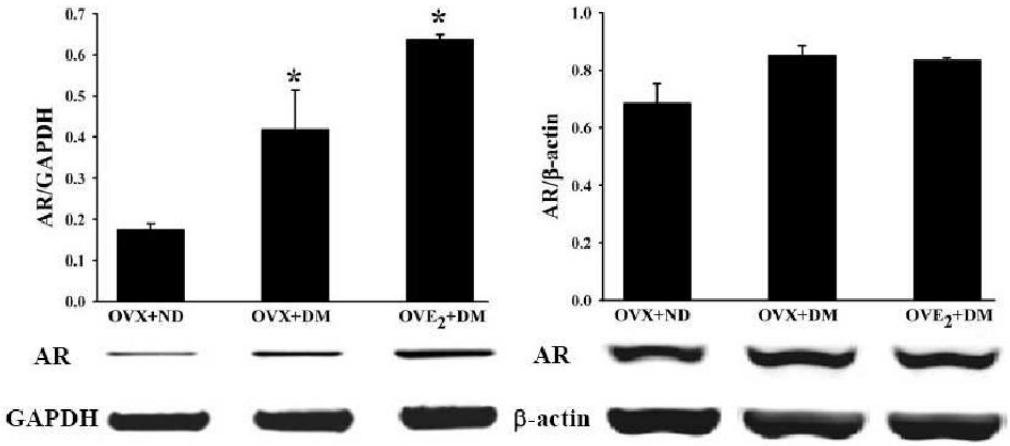

Fig 5.

Effect of estrogen replacement therapy (ERT) on aldose reductase (AR) mRNA (left panel) and protein expression (right panel) in cortical samples of non-diabetic (ND) rats and rats with diabetes mellitus (DM). The bands in the lower portion of the left panel, represent typical mRNA signals for AR and GAPDH in OVX non-diabetic (OVX+ND) and OVX diabetic female rats in the absence (OVX+DM) or presence of ERT (OVE_2+DM). The upper portion of the left panel shows the quantification of AR mRNA abundance normalized against the GAPDH mRNA signal. Values are means ± SE; * $p < 0.05$ *vs* OVX+ND; n= 3 in each group. Representative Western immunoblots, depicting aldose reductase (~37 kDa) and β-actin (~ 42 kDa) expression, are provided in the lower portion of the right panel. The upper portion of the right panel shows the AR optical densities expressed relative to β-actin, in samples obtained from OVX+ND, OVX+DM, or OVE_2+DM rats. Using a one-way (Kruskal-Wallis) analysis of variance on ranks, a statistically significant difference ($p=0.04$) among the 3 groups was revealed. When applying a post-hoc test (Dunn's method) for group-to-group comparisons, no significant differences ($p>0.05$) were observed; n= 4 in each group.